ELSEVIER

Physica C 314 (1999) 73–80

PHYSICA C

Magnetic hysteresis of the zero-resistance critical temperature in YBaCuO, BiSrCaCuO and HgBaCaCuO superconducting polycrystals

A.J. Batista-Leyva [a,1], R. Cobas [a], M.T.D. Orlando [b], C. Noda [a], E. Altshuler [a,*]

[a] *Superconductivity Laboratory, IMRE - Physics Faculty, University of Havana, 10400 Havana, Cuba*

[b] *Physics Department, Universidade Federal do Espirito Santo, Vitoria, Brasil and Group of New Materials, CBPF, Rio de Janeiro, Brazil*

Received 16 March 1998; revised 5 August 1998; accepted 28 January 1999

Abstract

A comparative study of the hysteretical behavior of the zero resistance critical temperature for $YBa_2Cu_3O_{7-\delta}$, $(BiPb)_2Sr_2Ca_2Cu_3O_{10+\delta}$ and $(HgRe)Ba_2Ca_2Cu_3O_{8+\delta}$ superconducting ceramics was performed at low magnetic fields (under 400 Oe). The results were compared with those obtained through the magnetic hysteresis of the critical current density, showing good agreement in most cases. The qualitative explanation of the observed hysteresis in terms of intragranular flux trapping of the superconducting grains satisfies YBaCuO and BiSrCaCuO materials, but modifications might be necessary in the case of HgBaCaCuO.

Keywords: Granular superconductivity; Electrical resistivity; Critical current density; Weak links; Mixed state; Lower critical field H_{c1}

1. Introduction

The study of the dependence of transport properties with the applied magnetic field in ceramic superconductors has proven to be a powerful tool in the understanding of a variety of characteristics of high temperature superconductors (HTc).

An important fraction of these studies have been devoted to the $J_c(B_a)$ dependence in polycrystalline HTc's, for instance $YBa_2Cu_3O_{7-\delta}$ [1] and $(BiPb)_2Sr_2Ca_2Cu_3O_{10+\delta}$ [2,3]. The qualitative model of Peterson and Ekin [4], further developed by Evetts and Glowacki [5] stated the theoretical basis for the explanation of $J_c(B_a)$ and related dependencies. This model, put on more quantitative roots by Altshuler et al. [1] and by Müller and Mathews [6] has been applied in the understanding of the hysteretical behavior of J_c in ceramic superconductors. Following that model, this behavior can be explained by the effect of the flux trapped by the superconducting grains on the intergrain weak links, which produces a different performance of the average effective field at the junctions for increasing and decreasing applied fields. This irreversibility of the effective field at the junctions is a fingerprint of the hysteresis of the intragranular magnetization, which is supposed to follow some critical state model [7,8].

Flores et al. [9] demonstrated that the zero-resistance critical temperature (T_z), which strongly de-

* Corresponding author. E-mail: jea@infomed.sld.cu

[1] On leave from Physics Department, Engineering Faculty, University of Holguín, Holguín 80100, Cuba.

0921-4534/99/$ - see front matter
PII: S0921-4534(99)00144-6

pends on the junctions characteristics also shows a hysteretical behavior in YBaCuO ceramics and pointed out the possibility of employing this phenomenon as a tool in the study of local fields at intergranular junctions. No further reports of hysteresis of T_z in this or in other HTc systems have been published, as far as we know.

In the present paper, the hysteretical behavior of T_z for $YBa_2Cu_3O_{7-\delta}$, $(BiPb)_2Sr_2Ca_2Cu_3O_{10+\delta}$ and $(HgRe)Ba_2Ca_2Cu_3O_{8+\delta}$ ceramics is reported. The results of the different systems are compared and qualitatively explained in terms of flux trapping by the superconducting grains.

The 'flux trapping curves' for T_z in the three systems are also reported for the first time, to our knowledge, and some intragranular parameters are extracted from them.

2. Experimental

All the samples were prepared by the ceramic route. The details of each system are given below.

– YBaCuO: High quality powders of Y_2O_3, $BaCO_3$ and CuO were mixed in stoichiometric proportions, being the ratios Y:Ba:Cu in the original powders 1:2:3. These raw materials were calcinated for 16 h at 900, 920 and 940°C. At the end of each step the powders were ground in a mill. After that, they were pressed into pellets at 300 MPa, sintered at 950°C for 24 h, and cooled down to room temperature at the rate of 1°C/min in air atmosphere. Bars of approximately $10 \times 1 \times 1$ mm^3 were cut from the pellets. The obtained onset critical temperature at zero magnetic field, defined as the temperature of the maximum of the derivative $d\rho/dT$, was 90 K.

– BiSrCaCuO: Powders of high purity of the starting materials Bi_2O_3, PbO_2, $SrCaO_3$, $CaCO_3$ and CuO were mixed in a stoichiometric ratio Bi:Pb:Sr:Ca:Cu of 1.6:0.4:2:2:3. The powders were thermally treated at 700, 750 and 800°C. At the end of each treatment, the pellets were manually ground. The powders were pressed into pellets at 400 MPa and the sintering was carried out at a temperature of 848°C for 48 h; the samples were cooled down to room temperature at a rate of 1°C/min in air. Bars of approximately $10 \times 1 \times 1$ mm^3 were cut from the as sintered pellets. The onset critical temperature at zero magnetic field was 105 K.

– HgBaCaCuO: $BaCO_3$, $CaCO_3$, CuO and ReO_4 high purity powders were prepared in a 2:2:3:0,18 stoichiometric mixture. The mixture was first homogenized in an agate mortar and thermally treated at 850°C for 12 h under oxygen flow. After this, the material was crushed in an agate mortar and pelletized under 1 GPa. The pellets were submitted to calcination at 930°C for 15 h under oxygen flow. The latter procedure was repeated two times crushing the mixture between calcination treatments. The precursors were then treated at 930°C for 12 h using 20% oxygen and 80% argon flow. High purity HgO was added to the final mixture and homogenized in an agate mortar. The powder was pelletized uniaxially under 1 GPa, using a vacuum pump to reduce the gas present inside the pellet. It was immediately introduced inside both a gold foil and inside a quartz tube of 0.9 mm inner diameter. The filling factor was 1.1 g/cm^3. The quartz tube was sealed under vacuum (10^{-2} Torr), and introduced inside a stainless steel tube which was then filled with 2 bar of argon. The latter was introduced into an isostatic pressure furnace with 40 bar of argon. The sample was heated at a rate of 300°C/h until 700°C, at 120°C/h until 850°C and hold at this temperature for 15 h [10]. Then the furnace was cooled down at 120°C/h to 30°C. Bars of approximately $7 \times 1 \times 1$ mm^3 were cut. The onset critical temperature at zero magnetic field was 132 K.

The T_z values were determined from the $\rho(T)$ curves. Those measurements were performed via the four-probe technique, employing an ac excitation signal at 81 Hz, and a lock-in amplifier with a maximum noise of 100 nV. The contacts were deposited with silver paint. In order to minimize self-field generated tails a bias current with an r.m.s. value as low as 0.35 mA was selected. An autotuning temperature controller Lake Shore 330 dynamically controlled the temperature. In all the cases, the curves were measured at an increasing temperature sweep rate of 2 K/min and the resolution in temperature was 0.1 K. The magnetic field was generated by a long solenoid and the sample was located in such a way that the applied field was perpendicular to the bias current. Measurements were performed up to a final temperature greater than the onset critical

temperature, to guarantee that the sample stood in normal state after each measurement, being 'erased' its magnetic history.

Three different regimes of magnetic excitation were applied.

Virgin curve: The sample was zero field cooled (ZFC) to 80 K and the desired value of magnetic field was set directly from zero. Then a $\rho(T)$ curve was measured.

Returning curves: The sample was ZFC to 80 K, a maximum value (H_m) was set, and after a few seconds, the field was decreased to the desired value. Then a $\rho(T)$ curve was measured. As for the $J_c(B_a)$ dependence [1–3], two different curves were measured: *unsaturated*, when the increase of the H_m causes variations in the shape of the curve, and *saturated*, when the increase of H_m does not affect the curve.

Flux trapping curve: The sample was ZFC to 80 K, the desired maximum field value was set and after few seconds, the field was turned off. Then a $\rho(T)$ curve was measured.

In all cases, the experimental curves had 500 points.

3. Results and discussion

3.1. Resistivity vs. temperature curves

In Fig. 1(a) Arrhenius plots of $\ln(\rho/\rho_0)$ vs. T for the YBaCuO ceramic are shown, being ρ_0 the resistivity at the point T_0 were the curves for different applied fields split. The magnetic field was set directly from zero after ZFC for each curve. In Fig. 1(b) and (c) are shown similar curves for BiSrCaCuO and HgBaCaCuO respectively. The point of splitting is the same for the non-normalized data, so it is not related to the normalization process. It is evident that the tails of the curves are not linear, which departs from the behavior reported for thin films [11,12] and single-crystals [13]. Flores et al. [9] employed the expression of Kim et al. [14] for fitting the experimental data on YBaCuO polycrystals. It has a structure similar to an Arrhenius law, but with a potential energy depending non-linearly on temperature:

$$\rho(H,T) = \rho_0 \exp\left\{-\frac{U(H,T)}{T}\right\} \quad (1)$$

where

$$U(H,T) = U_0(H)\left(\frac{T_0}{T} - 1\right)^{\alpha}. \quad (2)$$

In our work we employed these expressions, using a voltage definition for T_z such that $\ln(\rho_o/\rho_z) = 5$, being $\rho_z = \rho(T_z)$. Our choice for the exponent α was $\alpha = 2$, which fits into the range proposed in Ref. [15]. Fig. 1 shows the resulting fits for the three superconducting systems under study, when the field has been increased from zero after ZFC. The agreement between the experimental data and the fitting curves is remarkable, with coefficients of determination better than 0.975 in all the cases.

When comparing the curves for the different systems we must note that in the curve for BiSrCaCuO (Fig. 1(b)), the part of the transition not affected by the magnetic field (i.e., that dominated by intragrain dissipation according to Henning et al. [16]) does not show the sharp drop displayed by YBaCuO (Fig. 1(a)) and (to less extent) by HgBaCaCuO (Fig. 1(c)). It is interesting to note that for YBaCuO, the onset critical temperature, defined as the inflection point in the resistive transition, was found to be of about 90 K, not far from that obtained by López et al. [3] for samples cooled in oxygen atmosphere. Therefore, the low concentration of oxygen in the furnace during the cooling only slightly affected the onset critical temperature. This is roughly coherent with the results of [17]. On the other hand the intergrain component, originated from the presence of weak links [18] and responsible for the pronounced tails in the transition [16] is strongly affected. This will be analyzed in more detail in Section 3.2.

In the case of HgBaCaCuO, it is easy to note that the curves corresponding to high magnetic fields are almost straight though they also fit very well to Eqs. (1) and (2) with $\alpha = 2$. This indicates a stronger field dependence of $U_0(H)$ for HgBaCaCuO than for YBaCuO and BiSrCaCuO samples, at least within

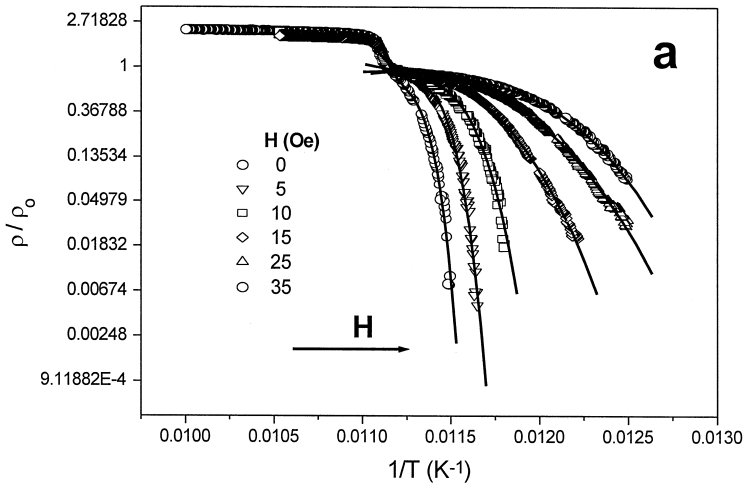
a
H (Oe)
0
5
10
15
25
35
H
ρ / ρo
2.71828
1
0.36788
0.13534
0.04979
0.01832
0.00674
0.00248
9.11882E-4
0.0100
0.0105
0.0110
0.0115
0.0120
0.0125
0.0130
1/T (K-1)

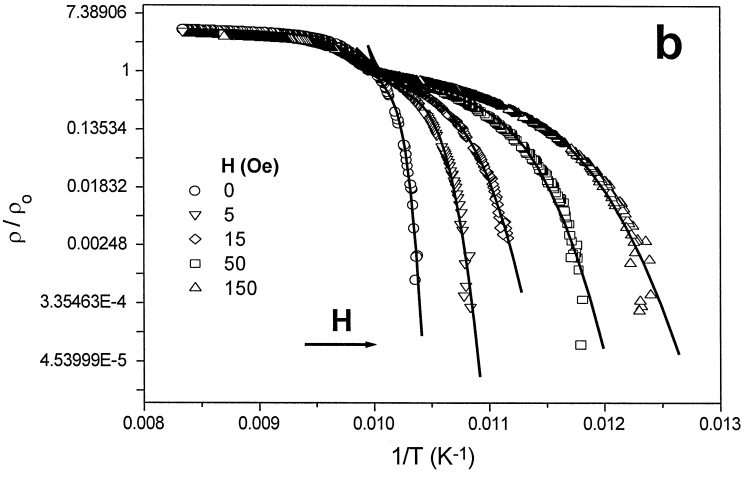
b
H (Oe)
0
5
15
50
150
H
ρ / ρo
7.38906
1
0.13534
0.01832
0.00248
3.35463E-4
4.53999E-5
0.008
0.009
0.010
0.011
0.012
0.013
1/T (K-1)

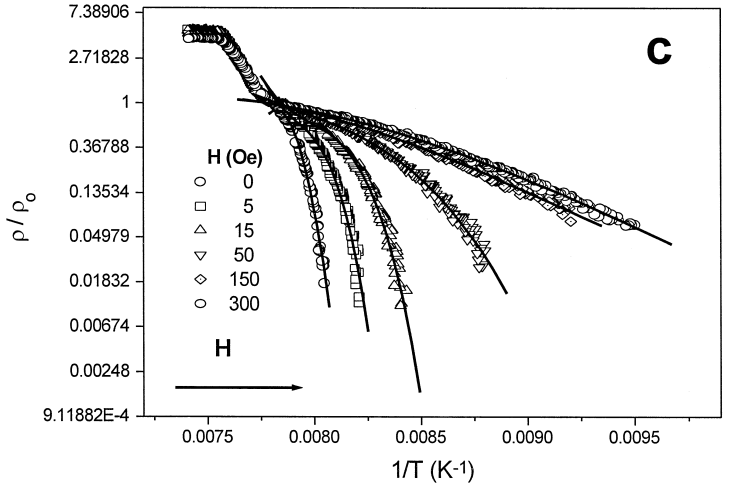
c
H (Oe)
0
5
15
50
150
300
H
ρ / ρo
7.38906
2.71828
1
0.36788
0.13534
0.04979
0.01832
0.00674
0.00248
9.11882E-4
0.0075
0.0080
0.0085
0.0090
0.0095
1/T (K-1)

the field range explored. This point deserves further attention and will be discussed elsewhere.

3.2. $T_z(H_a)$ curves

Fig. 2(a), (b) and (c) show the virgin curve and two ZFC returning curves, one saturated and the other unsaturated, for YBaCuO, BiSrCaCuO and HgBaCaCuO, respectively.

The curves obtained for YBCO samples (Fig. 2(a)) are in good agreement with those of Flores et al. [9] and reproduce the following characteristics, analogous to those reported by Altshuler et al. [1] for the dependence of the critical current density on the magnetic field for ceramic superconductors:

- The virgin curve has a maximum at some value $H_a = 0$, while the returning curves have a maximum at $H_a \neq 0$.
- With the increment of H_m, the maxima of the returning curves shift toward greater values of H_a, and the maximum values of $T_z(H)$ diminish.
- When increasing H_m, a saturation value is found H_{ms} such that for $H_m > H_{ms}$ there is no change in the shape of the returning curves.
- dT_z/dH_a is more pronounced in the virgin curve than in the returning ones; the greater the maximum field, the lower the slopes in the returning curves.

It is easy to note that the curves for BiSrCaCuO have a different behavior when compared with those for YBaCuO and HgBaCaCuO. The hysteresis, though present, is not pronounced for the BiSrCaCuO ceramics, and both the unsaturated and saturated returns are only slightly different from the virgin curves. This behavior agrees with that obtained for the hysteresis in critical current density by Muné et al. [2] and López et al. [3] in ceramic BiSrCaCuO samples processed through a similar route as ours. However, in their work, a noticeable reduction in the critical current was obtained, even for low maximum fields, being the critical current density at zero field of the saturated return a 40% of that corresponding to the virgin curve. In our case, the reduction in $T_z(0)$ for the saturated return (H_m = 400 Oe) is only a 4% of the $T_z(0)$ for the virgin curve, which corresponds to 4 K. Another distinctive characteristic of our curves is that the maxima of the returning curves are not obtained for $H_a = 0$ Oe, but for a value of 1–2 Oe. This is also in contrast with the reports of Refs. [2,3].

In those papers, a semi quantitative model was presented, based on the existence of regions with 'compressed', and with 'decompressed' magnetic fields for a given value of the applied field. Those percolative paths that cross links between grains reflecting the second situation show a 'soft' dependence of the critical current with the applied magnetic field, and are responsible for a zero field maximum and broad peaks. At the same time, the presence of percolative paths with compressed magnetic field forces the reduction in $J_c(H)$. In the present case, the situation seems to be different. Our measurements are made with a low bias current, so it is not difficult to find percolative paths including the 'less weak' links, in such a way that the reduction in T_z is not of the same magnitude as that in J_c.

The presence of the maximum for $H_a \neq 0$ in both returns is not completely clear. It can be related with the flux trapping in the superconducting grains, but this is partially in contradiction with the results of Schulz et al. [19]. Studying the behavior of the Meissner fraction with applied field in Bi 2223 ceramics, they found a maximum for the applied field of 2.5 G, in fair agreement with our results, but the authors attributed the phenomenon to the intergranular pinning rather than to the pinning inside the grains. Anyway, the evidence is not strong enough and this subject deserves further attention in future work, with the employment of magnetization measurements. Besides, the geometry of the samples of Refs. [2,3] was somewhat different and the difference in sample demagnetization must be taken into account for the explanation.

The curves for HgBaCaCuO samples (Fig. 2(c)) have a behavior similar to those obtained for YBaCuO, but the magnitude of the hysteretical effects is more pronounced. The virgin curve has a

Fig. 1. Arrhenius plots for (a) YBaCuO, (b) BiSrCaCuO and (c) HgBaCaCuO samples. The magnetic field was set directly from zero after ZFC. The continuous lines represent fits using Eqs. (1) and (2) (see text).

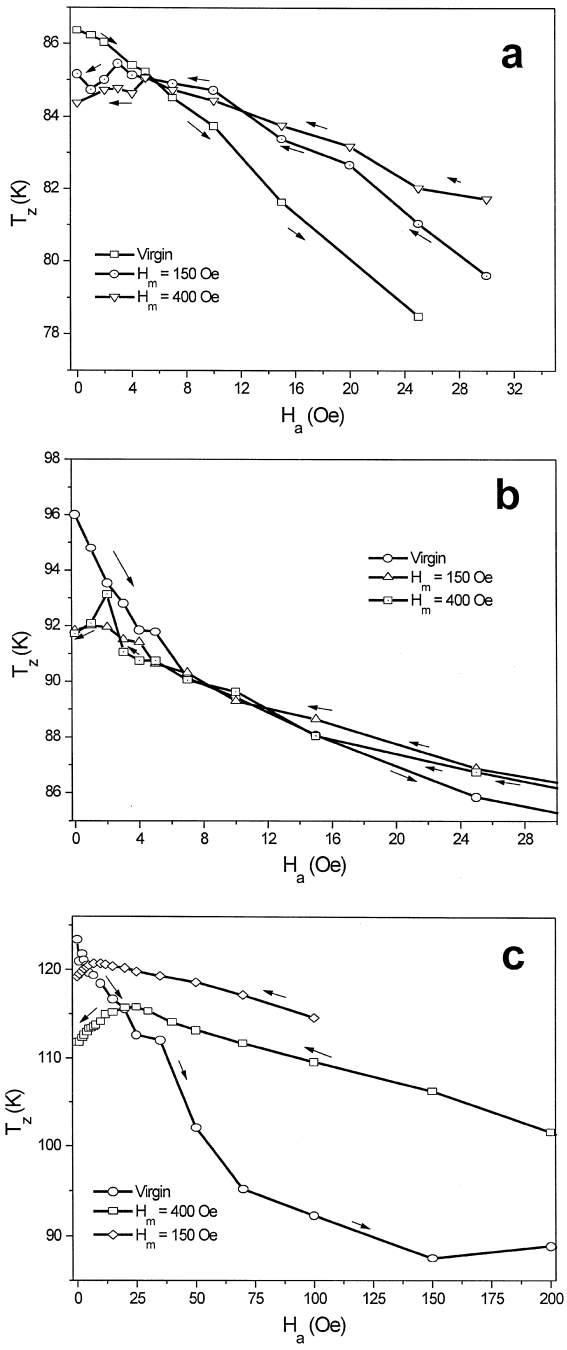

Fig. 2. Virgin and returning (unsaturated and saturated) curves for (a) YBaCuO, (b) BiSrCaCuO and (c) HgBaCaCuO samples. The lines are guides to the eye.

maximum variation $(T_z(0) - T_z(150))/T_z(0) \approx 0.25$, being 0.09 and 0.10 for YBaCuO and BiSrCaCuO respectively. The difference between the maximum of the saturated returning curve and its zero value is greater than 4 K. Finally, the reduction of $T_z(0)$ of the saturated return ($H_m = 400$ Oe) is a 9% of the $T_z(0)$ of the virgin curve and the maximum difference between the virgin curve and the saturated returning curve is 20 K (for $H_a = 150$ Oe).

Taking into account the fact that the grains of HgBaCaCuO have a plate-like shape [20,21], qualitatively similar to that of BiSrCaCuO, and that this shape seems to be responsible [2,3] for the differences between YBaCuO and BiSrCaCuO, it could be reasonable to expect a less pronounced hysteresis for HgBaCaCuO. This puzzling behavior will be investigated in more detail in the future.

3.3. Flux trapping curves, $T_z(0, H_m)$

The flux trapping curves in T_z for YBaCuO, BiSrCaCuO, and HgBaCaCuO are shown in Fig. 3(a), (b) and (c) respectively. These curves have been reported previously only for the hysteresis of the transport critical current density [2,17].

It is very important to notice that our curves do not have a trivial correspondence with similar curves for the critical current density, $J_c(0, H_m)$. A qualitative explanation of this fact is that the latter ones are measured at constant temperature while, in our case, the parameter that is related with the trapped flux (T_z) is measured by varying T. A typical process can be sketched as follows: at the temperature of 80 K, after a ZFC, the maximum field H_m is applied and then set to zero; if $H_m > H_{c1g}$ (where H_{c1g} is the effective first critical field of the grains), there is a certain amount of flux trapped by the grains. When the temperature grows, J_{cg} (the intragranular critical current density) lowers so, according to Bean's model [7], the trapped flux is also reduced. This means that at the beginning of the dissipation process, there is less flux inside the grains and their magnetic influence on the transport process at the weak links will be lower. On the other hand, because of the lowering of T_z with the increase of the applied field (provided that $H_a > H_{cig}$) this effect will be less noticeable as the applied field increases, because a minor part of the flux had been expelled due to the increase of temperature. This implies that, firstly, that the values of H_{c1g} and H_s extracted from the T_z flux trapping

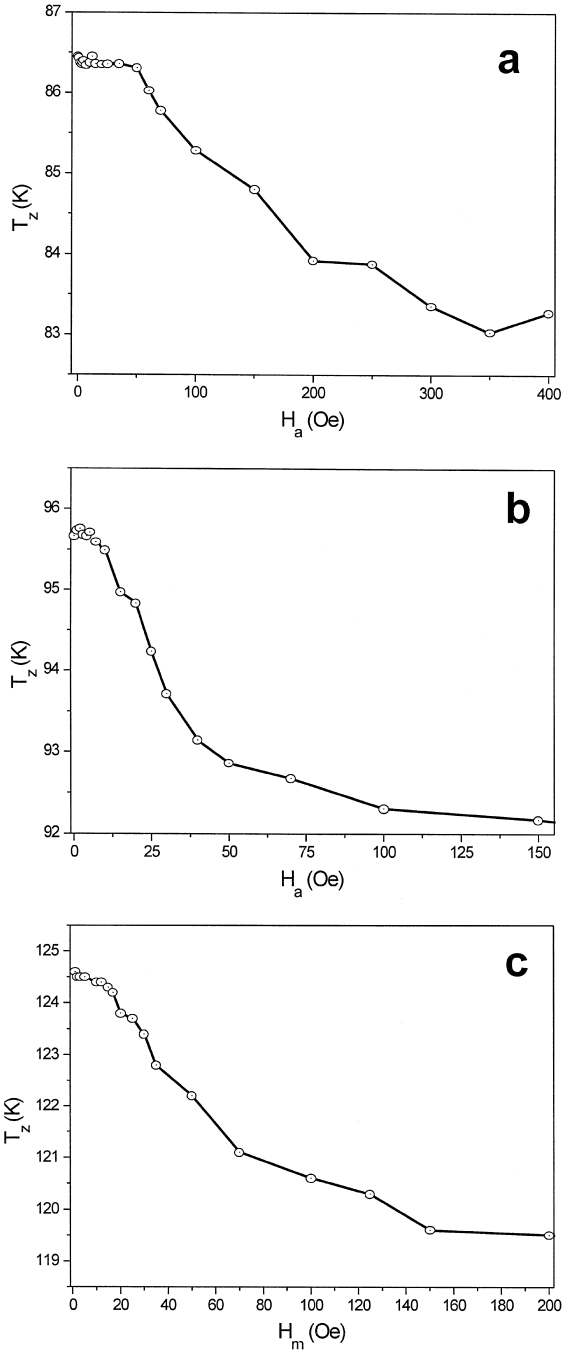

Fig. 3. Flux trapping curves for (a) YBaCuO, (b) BiSrCaCuO and (c) HgBaCaCuO samples. The lines are guides to the eye.

curve correspond to the temperature at which H_m was applied (i.e., 80 K in our case), and secondly, that the shape of the curve between these fields (particularly in the neighborhood of H_{c1g}) would differ from the J_c flux trapping analogue.

For YBaCuO, $H_{c1g} \approx 50$ Oe and $H_s \approx 250$ Oe at 80 K. Both values can be used in order to calculate the full penetration field $H^* = (H_s - H_{c1g})/2$ [22], which resulted in $H^* \approx 100$ Oe at 80 K. The H_{c1g} value is in good agreement with that obtained by Altshuler et al. [17,22] at liquid nitrogen temperature using two different methods: the flux trapping curve of J_c and vibrating sample magnetometry. Our value of H^* is less than 20% greater than that of Ref. [22]. It is important to realize that our samples are partially deoxygenated and the comparison with oxygenated ones is doubtful, but in Refs. [17,22] it is demonstrated that the oxygen content affects chiefly the junctions, and in a lesser degree the intrinsic characteristics of the grains, being the shape of the flux trapping curves for an as sintered sample reasonable similar to that obtained after a moderate deoxygenation thermal treatments in air atmosphere.

For BiSrCaCuO, $H_{c1g} \approx 10$ Oe, and $H_s \approx 100$ Oe at 80 K. These values are in good agreement with those obtained by López et al. [3] using $J_c(0, H_m)$ measurements. The value obtained for H^* (45 Oe) is in good agreement with Ref. [3] (42 Oe) which was also determined via J_c. Finally, for HgBaCaCuO, we obtained $H_{c1g} \approx 15$ Oe, while $H_s \approx 150$ Oe that yields $H^* \approx 70$ Oe at 80 K. In this case, no reference to compare with was available.

4. Conclusions

The magnetic irreversibility in T_z for three HTc ceramic systems has been studied. In all the samples the zero resistance critical temperature showed to depend on its magnetic history, displaying common features that can be qualitatively explained through the flux trapping model introduced by Evetts and Glowacki [5] and extended by Altshuler et al. [1] and Müller and Mathews [6]. For the BiSrCaCuO sample, maxima in returning curves are obtained for non-zero values of the applied field; this effect had not been reported in the analogous hysteresis of J_c. The behavior of the curves for the HgBaCaCuO sample is quite similar to the YBaCuO ones, in partial contradiction with the model of Muné et al. [2] and López et al. [3], from which one might expect that its behavior must resemble that of BiSrCaCuO.

The zero-resistance critical temperature flux trapping curves for HTc polycrystals were reported by the first time, and demonstrated to be consistent with the critical current density flux trapping ones reported earlier for the YBaCuO system. It is important to note that the intragrain magnetic parameters extracted from the former characteristics correspond to the temperature at which the maximum fields are applied.

Acknowledgements

M.T.D. Orlando acknowledges the financial support from CNPq, FINEP, CAPES, CST, CVD and UFES, and thanks Dr. E. Baggio-Saitovich, Head of the Group of New Materials at CBPF. We also acknowledge the financial support granted by the Third World Academy of Sciences through research project 95-124 RG/PHYS/LA.

References

[1] E. Altshuler, J. Musa, J. Barroso, A.R.R. Papa, V. Venegas, Cryogenics 33 (1993) 308.
[2] P. Muné, E. Altshuler, J. Musa, S. García, R. Riera, Physica C 226 (1994) 12.
[3] J. López, P. Muné, S. García, E. Altshuler, Physica C 272 (1996) 13.
[4] R.L. Peterson, W. Ekin, Phys. Rev. B 37 (1988) 9848.
[5] J.E. Evetts, B.A. Glowacki, Cryogenics 28 (1988) 641.
[6] K.H. Müller, D.N. Mathews, Physica C 206 (1993) 275.
[7] C.P. Bean, Rev. Mod. Phys. 36 (1964) 31.
[8] Y.B. Kim, C.F. Hempstead, A.R. Strnad, Phys. Rev. 129 (1962) 528.
[9] L.E. Flores, E. Altshuler, S. García, J. Musa, Physica C 234 (1994) 368.
[10] A. Sin, A.G. Cunha, A. Calleja, M.T.D. Orlando, F.G. Emmerich, E. Baggio-Saitovich, S. Piñol, J.M. Chimenos, X. Obradors, Physica C 306 (1998) 34.
[11] X.G. Xiu, B. Wuyts, M. Maenhoudt, V.V. Malshalkov, Y. Bruynseraede, Phys. Rev. B 52 (1995) 1559.
[12] J.T. Kucera, T.P. Orlando, G. Virshup, J.N. Eckstein, Phys. Rev. B 46 (1992) 11004.
[13] T.T.M. Palstra, B. Batlogg, L.F. Schneemeyer, J.V. Waszczak, Phys. Rev. Lett. 61 (1988) 14, 1662.
[14] D.H. Kim, K.E. Gray, R.T. Kampwirth, D.M. McKay, Phys. Rev. B 42 (1990) 6249.
[15] S.X. Dou, H.K. Liu, Supercond. Sci. Technol. 6 (1993) 297.
[16] T. Henning, H. Kliem, A. Weyers, W. Bauhofer, Supercond. Sci. Technol. 10 (1997) 721.
[17] E. Altshuler, S. García, J. Barroso, Physica C 177 (1991) 61.
[18] K. Moorjani, B.F. Kim, J. Bohandy, F.J. Adrian, International Conference on Superconductivity-ICSC. S.K. Joshi, C.N.R. Rao, V. Subramanyan (Eds.), World Sci. Press. Singapore, 1990, 170.
[19] B. Schulz, B. Schliepe, W. Wisny, K. Baberschke, Physica C 199 (1992) 356.
[20] A. Tokiwa-Yamamoto, K. Isawa, M. Itoh, S. Adachi, H. Yamamuchi, Physica C 216 (1993) 250.
[21] K. Isawa, A. Tokiwa-Yamamoto, M. Itoh, S. Adachi, H. Yamamuchi, Physica C 217 (1993) 11.
[22] E. Altshuler, Ph.D. Thesis, University of Havana, Havana, 1994.